Plate Motion Parameters Estimated from Changing Rate of VLBI and SLR Baseline Lengths

Tôhoku Geophys. Journ. (Sci. Rep. Tôhoku Univ., Ser. 5), Vol. 32, Nos. 3, 4, pp. 107-126, 1990 107

Plate Motion Parameters Estimated from Changing Rates of VLBI and SLR Baseline Lengths

KACHISHIGE SATO

Division of Earth Rotation, National Astronomical Observatory, Mizusawa, Iwate 023

(Received December 26, 1989)

Abstract: Changing rates of VLBI and SLR baseline lengths are inverted with a least squares method to estimate plate motion parameters. We assume that these changes of the baseline lengths are entirely due to horizontal motions of rigid plates on the earth's surface. Fixing the parameters of the Pacific plate to those of the AM1-2 model of Minster and Jordan, we seek for those of the North American and Eurasian plates. The VLBI and SLR data sets are separately inverted, since these two data sets do not have the same precision.

Some difference exists between the results obtained independently from the VLBI and SLR data sets. Furthermore, the plate motion parameters derived from both the data sets are quite different from those of the AM1-2 model. The AM1-2 model is considered to give the parameters averaged over a geological time scale, that is, a few million years. On the other hand, the parameters obtained here by inversions of the VLBI and SLR data sets are appropriate to very recent years. Thus the differences between the parameters obtained here and those of the AM1-2 model suggest that the plate motions in recent years are different from those averaged over a geological time span.

1. Introduction

In the last decade, new techniques such as the very long baseline interferometry (VLBI) and the satellite laser ranging (SLR) have been intensively applied to precise measurements of positions on the earth's surface. Many authors (*e.g.*, Christodoulidis *et al.*, 1985; Kondo *et al.*, 1986; Heki *et al.*, 1987, 1989; Murata, 1988; Ma *et al.*, 1989; Heki, 1989) have published changing rates of baseline lengths obtained by means of these techniques. The techniques have presently made it possible to measure the length of a baseline between two stations several thousands of kilometers away from each other with an accuracy of a few centimeters (Carter and Robertson, 1989). It is, therefore, expected that the plate motions which are considered to be as fast as several cm/yr in speed are observable by VLBI and SLR.

There are considerable papers (*e.g.*, Christodoulidis *et al.*, 1985; Kondo *et al.*, 1986; Heki *et al.*, 1987, 1989; Murata, 1988; Ma *et al.*, 1989; Heki, 1989) comparing the changing rates of VLBI or SLR baseline lengths with those expected from certain plate motion models such as the AM1-2 model of Minster and Jordan (1978). Very few authors, however, estimated the plate motion parameters by inverting the changing rates data of VLBI or SLR baseline lengths. Kondo *et al.* (1986) estimated the parameters of the Pacific plate from changing rates data of 10 VLBI baseline lengths, fixing the

parameters of the North American and Eurasian plates to those of the AM1-2 model. Heki *et al.* (1989) estimated the relative plate motion parameters between the North American and Pacific plates together with a uniform contraction rate of baselines, using 15 changing rates data of VLBI baseline lengths. However, the numbers of data used in these two papers do not seem enough to obtain meaningful results.

All of the plate motion models ever presented such as the AM1-2 model are derived from combined data sets including spreading rates at ocean ridges, azimuths of transform faults and seismic slip vectors. These models are thus considered to give the parameters averaged over a geological time scale, say, a few million years. However, the plate motion parameters in a short period may be different from those averaged over a long time scale. Therefore, it is desirable to derive the plate motion parameters compatible with VLBI and SLR data.

In this paper, we seek for the plate motion parameters by inverting the changing rates of VLBI and SLR baseline lengths with a least squares method and compare them with those of the AM1-2 model.

2. Mathematical Formulation

In this section, descriptions are briefly given for the derivation of observational equations and for the method of inversion in the sense of least squares. We assume that the earth is a sphere and the plates rigidly move only in horizontal direction on the earth's surface. The effect of ellipticity of the earth on the changing rates of baselines is much smaller than present observational error of VLBI and SLR. Therefore, the assumption of spherical earth does not significantly affect the results.

2.1. Derivation of Observational Equations

It is well known that the motion of each plate can be regarded as a rotation on the earth's surface with respect to a certain pole (Euler motion) (*e.g.*, Chase, 1972 ; Minster *et al.*, 1974).

We consider N_p plates and seek for the rotation pole position and the rotation rate of each plate. Let the pole position of the k-th plate be $P_k(\Phi_k, \Lambda_k)$, where Φ_k and Λ_k mean the latitude and longitude, respectively, and its rotation rate be Ω_k (positive value implies clockwise rotation of the plate as to be seen from the center of the earth).

Let $\boldsymbol{x}_s=(x_s,y_s,z_s)^t$ be the position vector of observational station-s whose latitude and longitude are ϕ_s and λ_s, respectively. x, y and z are the usual Cartesian coordinates with the earth's center as the origin. t means transposition.

We consider the position vectors of two stations, *i.e.*, station-a on plate-k and station-b on plate-l, before and after displacement caused by plate motions. These vectors are denoted by $\boldsymbol{x}_a=(x_a, y_a, z_a)^t$ and $\boldsymbol{x}_b=(x_b, y_b, z_b)^t$, before displacement, and $\boldsymbol{x}'_a=(x'_a, y'_a, z'_a)^t$ and $\boldsymbol{x}'_b=(x'_b, y'_b, z'_b)^t$, after displacement, respectively.

The Cartesian components of $\boldsymbol{x}_a$ and $\boldsymbol{x}_b$ are given by

$$\left.\begin{aligned} x_c &= R_e \cos\phi_c \cos\lambda_c, \\ y_c &= R_e \cos\phi_c \sin\lambda_c, \\ z_c &= R_e \sin\phi_c, \end{aligned}\right\} \tag{1}$$

where c is either a or b, and R_e is the radius of the earth.

The position vectors $\boldsymbol{x}'_a$ and $\boldsymbol{x}'_b$ can be easily obtained by the Euler transformations of $\boldsymbol{x}_a$ and $\boldsymbol{x}_b$, respectively (*e.g.*, Goldstein, 1980). These vectors are given by

$$\boldsymbol{x}'_c = \boldsymbol{F}_q \boldsymbol{x}_c, \tag{2}$$

where c is again either a or b, and $q=k$ when $c=a$ whereas $q=l$ when $c=b$. Here

$$\boldsymbol{F}_q = \begin{pmatrix} f_{11}(\Phi_q, \Lambda_q, \Omega_q) & f_{12}(\Phi_q, \Lambda_q, \Omega_q) & f_{13}(\Phi_q, \Lambda_q, \Omega_q) \\ f_{21}(\Phi_q, \Lambda_q, \Omega_q) & f_{22}(\Phi_q, \Lambda_q, \Omega_q) & f_{23}(\Phi_q, \Lambda_q, \Omega_q) \\ f_{31}(\Phi_q, \Lambda_q, \Omega_q) & f_{32}(\Phi_q, \Lambda_q, \Omega_q) & f_{33}(\Phi_q, \Lambda_q, \Omega_q) \end{pmatrix}, \tag{3}$$

where

$$\left.\begin{aligned} f_{11}(\Phi, \Lambda, \Omega) &= \cos^2\Phi \cos^2\Lambda(1-\cos\Omega)+\cos\Omega \\ f_{12}(\Phi, \Lambda, \Omega) &= \cos^2\Phi \sin\Lambda \cos\Lambda(1-\cos\Omega)-\sin\Phi \sin\Omega, \\ f_{13}(\Phi, \Lambda, \Omega) &= \sin\Phi \cos\Phi \cos\Lambda(1-\cos\Omega)+\cos\Phi \sin\Lambda \sin\Omega, \\ f_{21}(\Phi, \Lambda, \Omega) &= \cos^2\Phi \sin\Lambda \cos\Lambda(1-\cos\Omega)+\sin\Phi \sin\Omega, \\ f_{22}(\Phi, \Lambda, \Omega) &= \cos^2\Phi \sin^2\Lambda(1-\cos\Omega)+\cos\Omega, \\ f_{23}(\Phi, \Lambda, \Omega) &= \sin\Phi \cos\Phi \sin\Lambda(1-\cos\Omega)-\cos\Phi \cos\Lambda \sin\Omega, \\ f_{31}(\Phi, \Lambda, \Omega) &= \sin\Phi \cos\Phi \cos\Lambda(1-\cos\Omega)-\cos\Phi \sin\Lambda \sin\Omega, \\ f_{32}(\Phi, \Lambda, \Omega) &= \sin\Phi \cos\Phi \sin\Lambda(1-\cos\Omega)+\cos\Phi \cos\Lambda \sin\Omega, \\ f_{33}(\Phi, \Lambda, \Omega) &= \sin^2\Phi(1-\cos\Omega)+\cos\Omega. \end{aligned}\right\} \tag{4}$$

Then we obtain the observational equation describing the changing rate of the baseline length between station-a on plate-k and station-b on plate-l:

$$\Delta l_{a,b}^{(obs)} \simeq |\boldsymbol{F}_k \boldsymbol{x}_a - \boldsymbol{F}_l \boldsymbol{x}_b| - |\boldsymbol{x}_a - \boldsymbol{x}_b|, \tag{5}$$

where $\Delta l_{a,b}^{(obs)}$ is observed changing rate, and '$\simeq$' means that the left-hand-side includes an observational error.

We can also calculate the azimuth (Θ_a) and rate (D_a) of displacement of station-a respectively from

$$\Theta_a = \cos^{-1}\left\{\frac{\sin\phi'_a - \sin\phi_a \cos\Delta_{a,a'}}{\cos\phi_a \sin\Delta_{a,a'}}\right\} = \sin^{-1}\left\{\frac{\sin(\lambda'_a-\lambda_a)\cos\phi'_a}{\sin\Delta_{a,a'}}\right\}, \tag{6}$$

and

$$D_a = |\boldsymbol{F}_k \boldsymbol{x}_a - \boldsymbol{x}_a|, \tag{7}$$

where

$$\left.\begin{aligned} &\phi'_a = \sin^{-1}(z'_a/R_e), \\ &\lambda'_a = \cos^{-1}\{x'_a/(R_e\cos\phi'_a)\} = \sin^{-1}\{y'_a/(R_e\cos\phi'_a)\}, \\ &\cos\Delta_{a,a'} = \cos\phi_a \cos\phi'_a \cos(\lambda_a-\lambda'_a)+\sin\phi_a \sin\phi'_a, \\ &\sin\Delta_{a,a'} = [1-\{\cos\phi_a \cos\phi'_a \cos(\lambda_a-\lambda'_a)+\sin\phi_a \sin\phi'_a\}^2]^{1/2}. \end{aligned}\right\} \tag{8}$$

2.2. Inversion by a Least Squares Method

We employ a usual linearized, iterative and weighted least squares method to invert the changing rates data of VLBI and SLR baseline lengths.

We can arbitrarily choose a reference frame in the inversion problem of VLBI or SLR baseline length data. Since an obvious and simple way to specify a reference frame is to give the parameters of one of the plates, the parameters of the N_p-th plate are fixed to those of a certain reference model ever presented. In this study, we choose the AM1-2 model as the reference model, so that our reference frame coincides with that of the AM1-2 model. Then we will compare our parameters obtained by inversions of the VLBI and SLR data with those of the AM1-2 model.

The model vector $\boldsymbol{m}$ has, therefore, $3(N_p-1)$ independent components to be estimated:

$$\boldsymbol{m}=(\Phi_1,\ \Lambda_1,\ \Omega_1,\ \Phi_2,\ \Lambda_2,\ \Omega_2,\ \ldots\ldots,\ \Phi_{N_p-1},\ \Lambda_{N_p-1},\ \Omega_{N_p-1})^t. \tag{9}$$

First of all, we set an initial model vector $\boldsymbol{m}^{(0)}$ to that of the AM1-2 model and then iteratively improve the model vector by using the linearized observational equations:

$$\boldsymbol{W}^{1/2}\boldsymbol{A}^{(m)}\Delta\boldsymbol{m}^{(m)}=\boldsymbol{W}^{1/2}\Delta\boldsymbol{d}^{(m)}, \tag{10}$$

where $\boldsymbol{A}$ and $\boldsymbol{W}$ are the Jacobian matrix of $\boldsymbol{F}_q$ and weighting matrix, respectively (Nakagawa and Oyanagi, 1982). $\Delta\boldsymbol{m}^{(m)}$ and $\Delta\boldsymbol{d}^{(m)}$ are a correction vector to the model vector $\boldsymbol{m}$ and a residual vector, respectively, at the m-th step of improvement of the model vector. The elements of the Jacobian matrix $\boldsymbol{A}$ are given in Appendix. The weighting matrix $\boldsymbol{W}$ has diagonal elements equal to the reciprocals of the variances of observed changing rates. All of non-diagonal elements are set to zero, since we assume that all of covariances of observed changing rates are equal to zero.

By solving (10), we obtain $\Delta\boldsymbol{m}^{(m)}$ and can improve the model vector to obtain a new one, *i.e.*, $\boldsymbol{m}^{(m)}=\boldsymbol{m}^{(m-1)}+\alpha\Delta\boldsymbol{m}^{(m)}$. Here α is a reduction factor for the correction vector, which is usually set to one in this study. This improvement of the model vector is continued till a stationary one is attained.

We solve the observational equations (10) by performing a QR-decomposition of the weighted Jacobian matrix. This matrix can be decomposed with, for example, usual Householder transformations (*e.g.*, Wilkinson and Reinsch, 1971) to give

$$\boldsymbol{W}^{1/2}\boldsymbol{A}^{(m)}=\boldsymbol{Q}\boldsymbol{R}, \tag{11}$$

where $\boldsymbol{Q}$ is an orthogonal matrix and $\boldsymbol{R}$ an upper triangular matrix. By substituting (11) into (10), we obtain a set of linear equations:

$$\left.\begin{aligned}\boldsymbol{Z}^{(m)}&=\boldsymbol{Q}^t\boldsymbol{W}^{1/2}\Delta\boldsymbol{d}^{(m)},\\ \boldsymbol{R}\Delta\boldsymbol{m}^{(m)}&=\boldsymbol{Z}^{(m)}.\end{aligned}\right\} \tag{12}$$

Thus we can solve (10) to obtain

$$\Delta\boldsymbol{m}^{(m)}=\boldsymbol{R}^{-1}\boldsymbol{Z}^{(m)}=\boldsymbol{R}^{-1}\boldsymbol{Q}^t\boldsymbol{W}^{1/2}\Delta\boldsymbol{d}^{(m)}. \tag{13}$$

3. Simulations with Artificial Data Sets

We make some simulations with artificial data sets before inversions of the actual VLBI and SLR data sets. The purpose of these simulations is to check our computer program as well as to investigate how observational errors affect the estimation of parameters. The method and results of simulations are described below.

The simulations are performed by using 19 stations and 135 baselines shown in Fig. 1.

Fifteen of these stations are the same as those in the 'LAGEOS SLR network for plate motion' described in Murata (1988). Unfortunately this network includes only one station respectively on each of the Indian and South American plates. It is impossible to obtain all components of the model vector if there is only one station on a plate because the coefficient matrix in the linear equations becomes singular. Therefore, we add four more stations so that there are three stations on each of these plates. Three of them are the SLR stations also appearing in Murata (1988) (*i.e.*, the NATMAP station on the Indian plate and the SNTAGO and CERTOL stations on the South American plate) and one is the VLBI station on the Tasmania Island (on the Indian plate) which recently became operational (Carter and Robertson, 1989). Consequently, the numbers of stations on each plate are three, four, six, three and three on the Pacific (PCFC), North

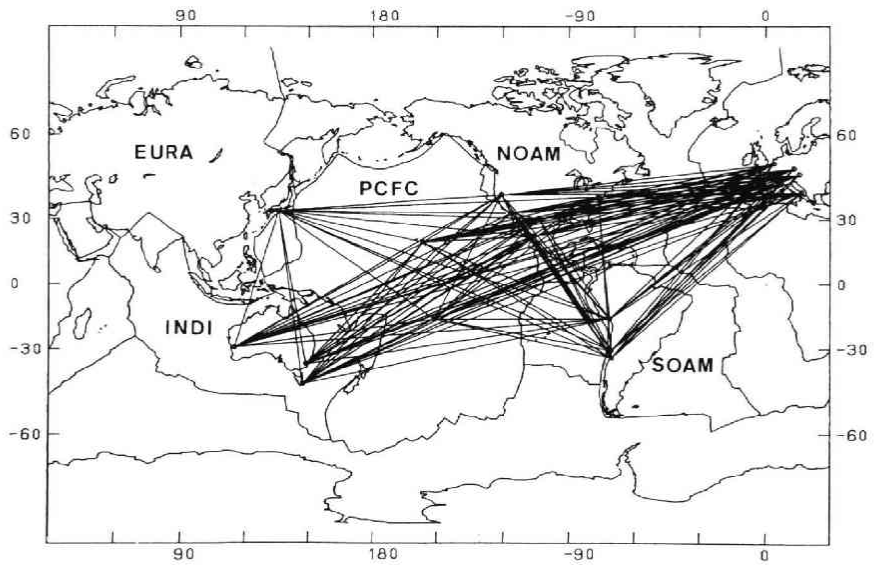

Fig. 1 Stations and baselines used in the simulations. Changing rates of 135 baseline lengths connecting 19 stations are used. 15 of these stations are the same as those in the 'LAGEOS SLR network for plate motion' described in Murata (1988) and the others are additionally employed. Approximate plate boundaries shown in figures are taken from Forsyth and Uyeda (1975). Abbreviations used in figures and tables are: PCFC, Pacific; EURA, Eurasian; NOAM, North American; SOAM, South American, and INDI, Indian plates, respectively.

American (NOAM), Eurasian (EURA), Indian (INDI) and South American (SOAM) plates, respectively. Hereafter abbreviated names of these plate will be used.

81 baselines out of 135 are the interplate baselines also described in Murata (1988) and the other 54 baselines are fictitious ones including the four additional stations.

The results of simulations are summarized in Table 1. In the table, Φ and Λ respectively mean the latitude and longitude of the rotation pole of each plate, and Ω is the rotation rate of each plate. For the simulations, we make a fictitious plate motion model where the parameters of each plate are set to the values presented in the rows denoted by 'given' in the table. Then we calculate the changing rate of each baseline length expected from this fictitious plate motion model.

Table 1. Estimated Plate Motion Parameters in the Simulations Made by Using 19 Stations and 135 Baselines Shown in Fig. 1.
Numeral in the parenthesis after each plate name is the number of stations on the respective plate. Φ, Λ and Ω respectively mean the latitude and longitude of the rotation pole and the rotation rate of each plate. One-sigma formal errors are also presented.

Plate	condition	Φ (°N)	Λ (°E)	Ω (deg/m.y.)
PCFC(3)	given	−70.00	110.00	0.900
NOAM(4)	given	−65.00	−30.00	0.400
	(O-C)≡0.	−65.00	−30.00	0.400
	S.D. of (O-C)=0.1 cm/yr	−65.01±0.71	−29.82±3.09	0.400±0.005
	S.D. of (O-C)=0.5 cm/yr	−64.37±3.70	−28.86±14.88	0.404±0.025
	S.D. of (O-C)=1.0 cm/yr	−62.35±8.03	−27.56±27.03	0.414±0.051
	S.D. of (O-C)=2.0 cm/yr	−56.43±17.00	−25.57±43.44	0.451±0.112
EURA(6)	given	5.00	−10.00	0.100
	(O-C)≡0.	5.00	−10.00	0.100
	S.D. of (O-C)=0.1 cm/yr	4.98±2.57	−10.02±3.16	0.100±0.005
	S.D. of (O-C)=0.5 cm/yr	4.48±12.77	−11.66±16.30	0.106±0.025
	S.D. of (O-C)=1.0 cm/yr	3.19±24.62	−15.83±33.01	0.123±0.051
	S.D. of (O-C)=2.0 cm/yr	1.57±37.14	−18.80±50.88	0.180±0.105
INDI(3)	given	30.00	45.00	0.650
	(O-C)≡0.	30.00	45.00	0.650
	S.D. of (O-C)=0.1 cm/yr	29.97±0.95	45.04±1.48	0.650±0.008
	S.D. of (O-C)=0.5 cm/yr	29.63±4.73	45.22±7.34	0.656±0.042
	S.D. of (O-C)=1.0 cm/yr	28.79±9.24	45.49±14.29	0.674±0.088
	S.D. of (O-C)=2.0 cm/yr	26.53±17.07	46.08±26.45	0.740±0.198
SOAM(3)	given	−70.00	60.00	0.300
	(O-C)≡0.	−70.00	60.00	0.300
	S.D. of (O-C)=0.1 cm/yr	−69.69±3.16	58.94±9.13	0.301±0.007
	S.D. of (O-C)=0.5 cm/yr	−63.90±14.18	46.32±40.64	0.322±0.045
	S.D. of (O-C)=1.0 cm/yr	−54.44±25.19	35.22±51.76	0.375±0.122
	S.D. of (O-C)=2.0 cm/yr	−40.11±35.41	26.35±53.39	0.526±0.313

First, we give these calculated changing rates of baseline lengths as observed data so that the residuals (*i.e.*, O-C) of the changing rates are exactly equal to zero. Giving the parameters of the AM1-2 model as the initial values, we search the least squares solution of the parameters in the manner described in the previous section. The obtained parameters of each plate are given in the rows denoted by '(O-C)$\equiv$0'. The parameters of PCFC are fixed to those of initially assumed model and are not estimated. It is found that the obtained parameters are precisely agree with those of our fictitious model. Therefore, we can say that the inversion perfectly reproduces the assumed model and our computer program is reliable.

Furthermore we make some additional simulations with data sets which are created so that the standard deviations of residuals of the changing rates are equal to 0.1, 0.5, 1.0 and 2.0 cm/yr, respectively. The residuals correspond to observational errors in the actual VLBI and SLR data. In order to create such data sets, we add Gaussian random errors to the calculated changing rates of baseline lengths. In these simulations, the mean values of the Gaussian random errors are equal to zero and their standard deviations are equal to 0.1, 0.5, 1.0 and 2.0 cm/yr, respectively.

For each simulation, we create independent 1000 data sets including the random errors thus generated and then invert them. Then the 1000 sets of obtained parameters are averaged to give a set of mean parameters for each simulation. The obtained parameters for each simulation are tabulated in the corresponding rows of the table. The estimated parameters of each plate fairly agree with those of the assumed model except for those of SOAM. The stations on SOAM are distributed only in the marginal region of the plate and do not scatter so much compared with those on other plates. This is the reason why the estimated parameters of SOAM do not agree well with those of the assumed model. In the table, the 1-sigma formal errors of estimated parameters are also presented. It is natural that the formal errors of estimated parameters grow as the standard deviations of residuals increase. The formal errors of estimated parameters are roughly in proportion to the standard deviations of residuals. Therefore, nonlinearity of our problem is not so strong. It is roughly said that if we want to determine the pole position and rotation rate of each plate with errors less than a few degrees and a few percent, respectively, the changing rates of baseline lengths must be determined with a standard deviation of observational errors as small as 0.1 cm/yr. Furthermore, stations on a plate must be distributed as uniformly as possible in order that observational errors do not affect so much the estimation of the plate motion parameters.

4. VLBI and SLR Data Sets Used for Inversions

In this section, given are some detailed descriptions of the VLBI and SLR data sets which are used for the inversions to estimate the plate motion parameters. We use the changing rates data and baseline lengths data which are presently available. The VLBI and SLR data sets are separately inverted because these two data sets do not have the same precision. These data sets inverted in the present study include the data of baselines related to only three plates, namely, NOAM, EURA and PCFC.

Table 2. Changing Rates of VLBI Baseline Lengths Used for the Estimation of the Plate Motion Parameters.

These are the mean rates for the period from 1983 to 1988. Original baseline length data are taken from Ma *et al.* (1989). Changing rates expected from the AM1-2 model (Minster and Jordan, 1978) in the case where the KASHIMA station belongs to NOAM are also given for comparison.

B.L. No.	Baseline	Number of Data	Rate (cm/yr)	AM1-2 Rate (cm/yr)
1	BLKBUTTE - VNDNBERG	10	2.40±0.31	4.26
2	FORT ORD - HATCREEK	6	−3.85±0.20	−4.45
3	FORT ORD - MOJAVE12	7	3.13±0.27	4.46
4	FORT ORD - OVRO 130	5	1.51±0.09	2.17
5	GILCREEK - KAUAI	38	−4.79±0.18	−4.96
6	GILCREEK - KWAJAL 26	14	−3.65±0.81	−2.25
7	GILCREEK - ONSALA 60	5	0.87±0.71	1.05
8	GILCREEK - VNDNBERG	35	−4.60±0.23	−5.21
9	GILCREEK - WETTZELL	8	1.45±0.70	1.01
10	HATCREEK - KAUAI	10	0.33±0.15	1.02
11	HATCREEK - MON PEAK	12	−2.93±0.33	−5.31
12	HATCREEK - PRESIDIO	7	−0.99±0.37	−3.79
13	HATCREEK - PT REYES	5	−2.10±0.36	−3.19
14	HATCREEK - VNDNBERG	33	−3.60±0.18	−4.88
15	HAYSTACK - ONSALA 60	98	1.09±0.12	1.73
16	HAYSTACK - WETTZELL	331	1.40±0.08	1.88
17	HRAS 085 - MON PEAK	23	3.19±0.18	4.08
18	HRAS 085 - ONSALA 60	57	0.32±0.30	1.49
19	HRAS 085 - VNDNBERG	28	3.43±0.22	4.23
20	HRAS 085 - WETTZELL	291	0.09±0.17	1.55
21	JPL MV1 - MOJAVE 12	18	0.51±0.16	−0.88
22	JPL MV1 - OVRO 130	15	−0.98±0.20	−4.46
23	JPL MV1 - PINFLATS	6	0.46±0.22	4.80
24	KASHIMA - KAUAI	36	−5.98±0.26	−7.74
25	KASHIMA - KWAJAL 26	12	−7.13±0.54	−8.54
26	KASHIMA - ONSALA 60	5	−3.92±1.84	−0.33
27	KASHIMA - VNDNBERG	17	−2.76±0.64	−4.26
28	KASHIMA - WETTZELL	8	−3.10±1.74	−0.41
29	KAUAI - MOJAVE 12	24	1.69±0.17	2.44
30	KWAJAL 26 - MOJAVE 12	15	0.91±0.87	2.54
31	MOJAVE 12 - MON PEAK	24	−2.38±0.16	4.72
32	MOJAVE 12 - ONSALA 60	14	−0.19±0.52	1.40
33	MOJAVE 12 - PBLOSSOM	8	0.22±0.15	−0.62
34	MOJAVE 12 - PRESIDIO	10	1.96±0.30	4.91
35	MOJAVE 12 - PT REYES	7	2.47±0.26	4.94
36	MOJAVE 12 - SANPAULA	5	1.47±0.44	0.83
37	MOJAVE 12 - VNDNBERG	89	1.86±0.08	2.15
38	MOJAVE 12 - WETTZELL	17	1.15±0.63	1.42
39	MON PEAK - OVRO 130	14	−2.52±0.21	−5.13
40	MON PEAK - QUINCY	7	−2.95±0.55	−5.32
41	MON PEAK - YUMA	8	2.76±0.22	3.35
42	NOME - VNDNBERG	7	−6.41±1.17	−5.29
43	ONSALA 60 - OVRO 130	8	−0.24±1.08	1.39
44	ONSALA 60 - RICHMOND	32	−0.09±0.47	1.56
45	ONSALA 60 - WESTFORD	84	0.87±0.14	1.73
46	OVRO 130 - PBLOSSOM	7	−0.83±0.25	−4.67
47	OVRO 130 - PRESIDIO	8	1.88±0.46	3.78
48	OVRO 130 - PT REYES	5	2.14±0.44	4.01
49	OVRO 130 - VNDNBERG	40	−0.80±0.14	−1.77
50	OVRO 130 - WETTZELL	7	0.23±1.07	1.41
51	PINFLATS - VNDNBERG	16	1.75±0.15	4.47
52	QUINCY - VNDNBERG	5	−3.07±0.61	−4.70
53	RICHMOND - WETTZELL	242	0.73±0.17	1.70
54	SOURDOGH - VNDNBERG	8	−4.97±0.90	−5.28
55	VNDNBERG - YUMA	15	3.66±0.39	4.52
56	WESTFORD - WETTZELL	307	1.25±0.09	1.88

4.1. VLBI Data Set Used for Inversions

We use the VLBI data such as the station coordinates and the baseline lengths presented in Ma *et al.* (1989).

From all available baselines, we use only the interplate baselines for which there are at least five observations spanning at least two years after 1983. We reject the HARTRAO station which is the only one on the African plate, since, as described previously, the problem is ill-conditioned when there is only one station on a plate. Consequently, the baselines between this station and other stations are removed. The baselines used in inversions are listed in Table 2 together with the numbers of observations and the changing rates of their lengths. The changing rates are obtained as the slopes of straight lines which fit best in the sense of least squares to the time series of the baseline length data. The positive and negative values imply expansion and contraction of the baselines, respectively. An example of baseline length change is illustrated in Fig. 2 for the baseline between the GILCREEK (on NOAM) and KAUAI (on PCFC) stations.

It is disputable on which plate the KASHIMA station, Japan, exists, on NOAM or EURA. This station is located near the southernmost tip of the northeastern Honshu, the Japanese main island, which used to be regarded as belonging to EURA (Chapman and Solomon, 1976). However, the station is recently considered to be included in

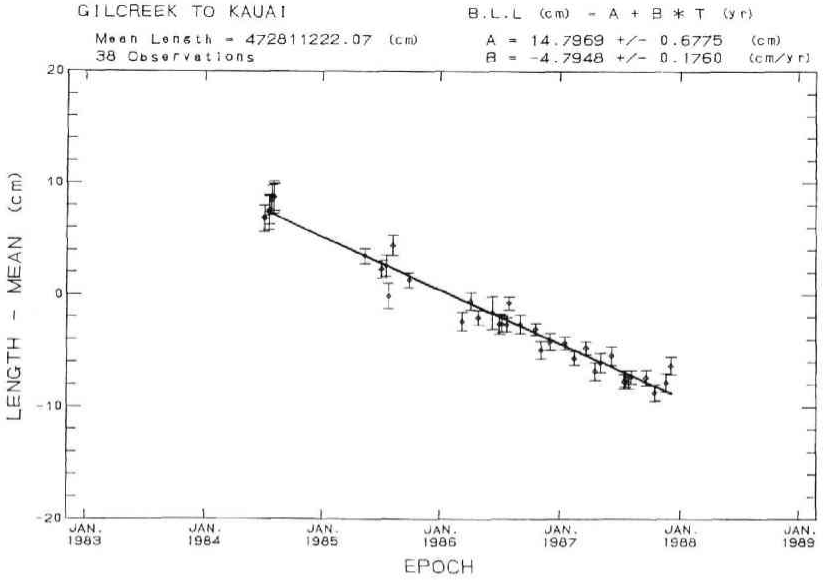

Fig. 2 Temporal change of the interplate baseline length between the GILCREEK (on NOAM) and KAUAI (on PCFC) stations. One-sigma error bars are attached to each data point. Straight line indicates the best-fit line to the observed lenghth data whose slope gives the chaniging rate of the baseline lenghth. Original baseline length data are taken from Ma *et al.* (1989).

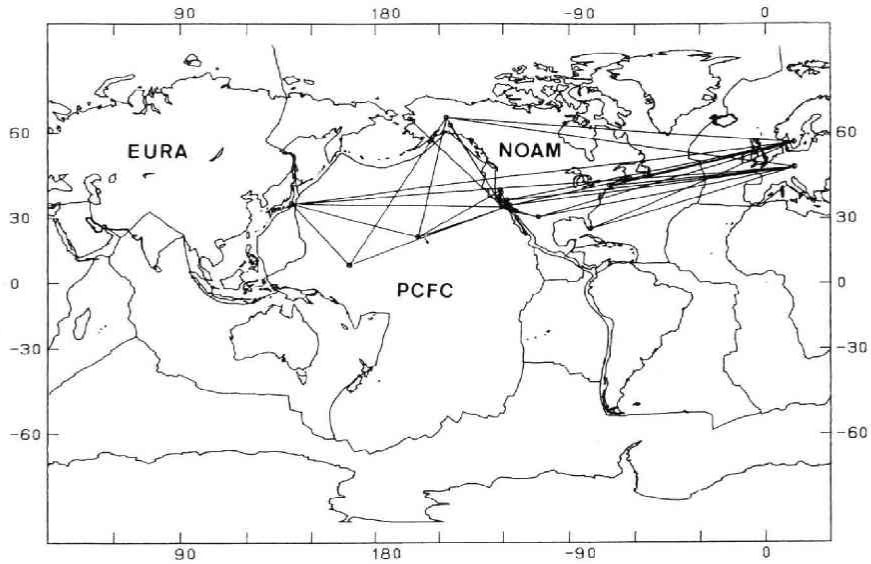

Fig. 3 VLBI stations and baselines used for the estimation of the plate motion parameters for the data set VLBI-56 (the KASHIMA station belongs to NOAM). 27 stations and 56 baselines are used in this case.

NOAM due to a new idea that the NOAM-EURA boundary lies in the Japan Sea to be connected to the Fossa Magna in central Honshu (Kobayashi, 1983 ; Nakamura, 1983). Therefore, we consider two cases : One is the case where the KASHIMA station belongs to NOAM, and the other to EURA. This station is located in a boundary region between two plates, being much affected by intraplate deformation (Heki, 1989). Thus we consider one additional case where the data set does not include this station.

The number of interplate baselines available depends on the case. There are 56, 59 and 51 baselines in the first, second and last cases, respectively. Hereafter the data sets corresponding to these cases will be called VLBI-56, VLBI-59 and VLBI-51, respectively. The stations and baselines in VLBI-56 (the KASHIMA station belongs to NOAM) are shown in Fig. 3.

For comparison, we also give in Table 2 the changing rates of baseline lengths expected from the AM1-2 model in the case where the KASHIMA station belongs to NOAM. It is readily found that almost all baseline lengths change at lower rates than the expected rates from the AM1-2 model. Although the reason for this is not clear at present, it is very interesting and important feature observed by VLBI.

4.2. SLR Data Set Used for Inversions

The SLR data are taken from Murata (1988). We use the stations and baselines in the 'LAGEOS SLR network for plate motion' mentioned previously. Because the stations on INDI and SOAM respectively are the only ones on each of these plates, these stations are rejected. Consequently, the baselines between these two stations and other

Table 3. Changing Rates of SLR Baseline Lengths Used for the Estimation of the Plate Motion Parameters.
These are the mean rates for the period from 1984 to 1986 taken from Murata (1988). Changing rates expected from the AM1-2 model (Minster and Jordan, 1978) are also given for comparison.

B.L. No.	Baseline	Rate (cm/yr)	AM1-2 Rate (cm/yr)
1	7086-7834	8.4± 9.0	1.6
2	7086-7835	2.2±12.9	1.7
3	7086-7838	−1.6± 2.0	−0.7
4	7086-7839	3.9± 8.9	1.5
5	7086-7840	3.9± 6.3	1.7
6	7086-7939	4.2± 8.0	1.5
7	7105-7834	6.8± 8.6	1.8
8	7105-7835	−0.1±11.4	2.0
9	7105-7838	0.3± 3.4	−0.4
10	7105-7839	1.9± 7.8	1.8
11	7105-7840	2.4± 6.6	1.9
12	7105-7939	2.4± 6.8	1.9
13	7109-7834	5.7± 6.4	1.4
14	7109-7835	0.2± 9.6	1.5
15	7109-7838	−2.5± 1.8	−0.9
16	7109-7839	1.9± 6.6	1.4
17	7109-7840	1.6± 6.4	1.5
18	7109-7939	2.1± 5.7	1.3
19	7122-7834	3.9± 7.1	1.5
20	7122-7835	−1.6± 9.7	1.6
21	7122-7838	−1.0± 1.7	−0.8
22	7122-7839	−0.1± 6.8	1.5
23	7122-7840	−0.1± 6.0	1.6
24	7122-7939	0.3± 5.8	1.5
25	7086-7110	1.6± 1.9	4.1
26	7086-7121	−3.8± 2.8	0.5
27	7086-7210	0.8± 2.1	3.1
28	7105-7110	2.2± 3.0	1.6
29	7105-7121	0.4± 2.2	1.0
30	7105-7210	2.3± 3.5	1.4
31	7109-7110	−3.2± 1.1	−5.3
32	7109-7121	−3.2± 2.4	−2.0
33	7109-7210	−0.7± 1.5	0.8
34	7122-7110	4.4± 1.4	5.4
35	7122-7121	2.4± 2.6	1.2
36	7122-7210	5.9± 1.7	4.4
37	7110-7834	4.4± 7.0	0.1
38	7110-7835	−0.9±10.0	0.6
39	7110-7838	−4.6± 1.7	−4.8
40	7110-7839	0.6± 6.9	0.1
41	7110-7840	0.5± 6.5	0.5
42	7110-7939	1.0± 6.0	0.3
43	7121-7834	1.3± 3.4	−0.5
44	7121-7835	−0.2± 4.4	0.1
45	7121-7838	−8.0± 2.4	−7.8
46	7121-7839	−0.2± 3.4	−0.6
47	7121-7840	0.1± 3.9	0.0
48	7121-7939	0.1± 2.5	−0.3
49	7210-7834	0.1± 4.5	−2.3
50	7210-7835	−3.1± 6.6	−1.7
51	7210-7838	−9.4± 1.9	−8.5
52	7210-7839	−2.0± 4.9	−2.4
53	7210-7840	−2.5± 5.5	−1.7
54	7210-7939	−2.0± 4.2	−2.2

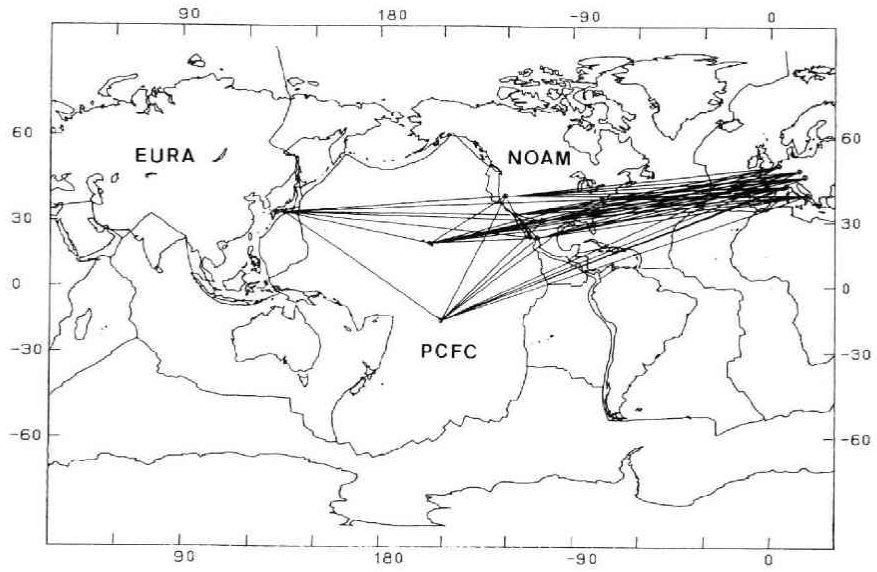

Fig. 4 SLR stations and baselines used for the estimation of the plate motion parameters for the data set SLR-54 (the SHO (7838) station is included). 13 stations and 54 baselines are used in this case.

stations are removed from the data set. Only interplate baselines are used, so that there are 54 available baselines. These baselines are listed in Table 3 together with the observed changing rates of their lengths and expected rates from the AM1-2 model. The positive and negative values again imply expansion and contraction of the baselines, respectively. We find here that, for about two-thirds of all baselines, the observed rates with SLR are larger than the expected rates in contradiction to those with VLBI. This is the most striking difference in the observed changing rates of baseline lengths between VLBI and SLR.

We consider two cases in the inversion of the SLR data set : One is the case where the SHO (Shimosato Hydrographic Observatory ; 7838) station, Japan, on EURA is included in the data set, and the other excluded. This exclusion of the SHO station is made because this station is also considered to be much affected by intraplate deformation as the KASHIMA station of VLBI (Sasaki, 1989). In the latter case, there are 12 stations and 47 baselines in all. Hereafter the data sets corresponding to these cases will be called SLR-54 and SLR-47, respectively.

The stations and baselines in SLR-54 (the SHO (7838) station is included) are shown in Fig. 4.

5. Plate Motion Parameters Estimated from the VLBI and SLR Data Sets

In this section, presented are the plate motion parameters estimated from the changing rates data of VLBI and SLR baseline lengths described in the previous section. We assume that the changes of baseline lengths are entirely caused by horizontal motions

of rigid plates. This means that we neglect the effects of vertical motions and internal deformation of the plates.

Due to an arbitrarity in choosing a reference frame, it is impossible to derive any absolute plate motion parameter only from the changing rates data of baseline lengths. Therefore, we fix the parameters of PCFC to those of the AM1-2 model and estimate the parameters of NOAM and EURA relative to the fixed parameters of PCFC. Parameters of other plates are not estimated here because there is none or insufficient number of stations on them. Since the parameters of PCFC are best estimated in the AM1-2 model except for those of the Cocos plate, PCFC is chosen as the reference plate.

As described in the previous section, we consider three and two cases, respectively, in the inversions of the VLBI and SLR data sets with respect to the treatments of the KASHIMA station in the VLBI data sets and of the SHO (7838) station in the SLR data sets.

The parameters estimated for each case are tabulated in Table 4 with those of the

Table 4. Estimated Plate Motion Parameters and Their 1-sigma Formal Errors for NOAM and EURA in Various Cases Where the Changing Rates of the VLBI (1983-1988) and SLR (1984-1986) Baseline Lengths are Inverted.
The parameters of PCFC are fixed to those of the AM1-2 model (Minster and Jordan, 1978). Φ, Λ and Ω respectively mean the latitude and longitude of the rotation pole and the rotation rate of each plate. One-sigma error ellipses are specified by the azimuth ζ_{max} of the major axis and the lengths $2\sigma_{max}$ and $2\sigma_{min}$ of the major and minor axes. The lengths of these axes are geocentric angles. The numbers of stations are those for each plate.

Plate	Data Set [No. of Sts.]	Plate Motion Parameter			Error Ellipse		
		Φ (°N)	Λ °(E)	Ω (deg/m.y.)	ζ_{max}	σ_{max} (deg)	σ_{min} (deg)
PCFC	(AM1-2)	−61.66± 5.11	97.19± 7.71	0.967±0.085	S16°E	5.23	3.50
NOAM	(AM1-2)	−58.31± 16.21	−40.67± 39.62	0.247±0.080	S57°E	23.12	12.14
	VLBI-56 [15] (KASHIMA∈NOAM)	−51.13± 4.61	−142.31± 2.54	0.300±0.004	S26°E	5.08	1.38
	VLBI-59 [14] (KASHIMA∈EURA)	−47.51± 5.49	−140.60± 2.60	0.301±0.005	S23°E	5.94	1.31
	VLBI-51 [14] (without KASHIMA)	−32.08± 5.52	−135.36± 1.74	0.320±0.013	S15°E	5.70	1.02
	SLR-54 [4] (with SHO, 7838)	−23.73± 54.12	−108.11± 15.03	0.383±0.254	N09°E	54.71	12.74
	SLR-47 [4] (without SHO, 7838)	−14.27± 46.21	−109.73± 12.27	0.443±0.345	S08°E	46.61	10.65
EURA	(AM1-2)	0.70±124.35	−23.19±146.67	0.038±0.057	S67°E	151.10	118.90
	VLBI-56[2] (KASHIMA∈NOAM)	30.68± 22.56	−116.92± 16.70	0.183±0.047	N36°E	27.52	5.56
	VLBI-59[3] (KASHIMA∈EURA)	−36.52± 4.11	−174.29± 6.46	0.278±0.019	N63°E	7.10	2.84
	VLBI-51[2] (without KASHIMA)	32.06± 15.62	−121.04± 11.38	0.269±0.052	S35°E	18.81	4.43
	SLR-54[6] (with SHO, 7838)	43.42± 36.46	−160.25± 78.64	0.182±0.240	S79°E	79.88	33.65
	SLR-47[5] (without SHO, 7838)	−43.06± 8.90	−168.48± 9.63	3.157±3.287	N48°E	12.40	4.27

AM1-2 model. The meanings of Φ, Λ and Ω are the same as those in Table 1. One-sigma formal errors and error ellipses are also presented. Reflecting the larger uncertainties of the changing rates data of SLR, the errors of estimated parameters are larger for the SLR data. Moreover, the errors of estimated parameters of EURA are generally larger than those of NOAM. The pole positions are depicted together with their approximate error ellipses in Figs. 5 and 6. These figures respectively correspond to the cases where the VLBI and SLR data sets are inverted. The error curves are ellipses if drawn in the plane tangent to the earth's surface at the corresponding pole. However, because of distortions introduced by the particular projection, the curves shown in these figures are not perfect ellipses. In these figures, the pole positions of the same plates in the AM1-2 model are also shown for comparison.

First, some difference exists between the parameters of each plate estimated independently from the VLBI and SLR data sets. However, the discrepancies in most of the parameters are not beyond the 1-sigma formal errors. The differences are rather larger in the parameters of NOAM. The discrepancies in the latitude and longitude of the rotation pole and the rotation rate of this plate estimated from theVLBI data sets and from the SLR data sets amount to about 20 degrees, 30 degrees and 0.1 deg/m.y., respectively.

Furthermore, neither the parameters obtained from the VLBI data sets nor those obtained from the SLR data sets consist with the parameters of the AM1-2 model. The

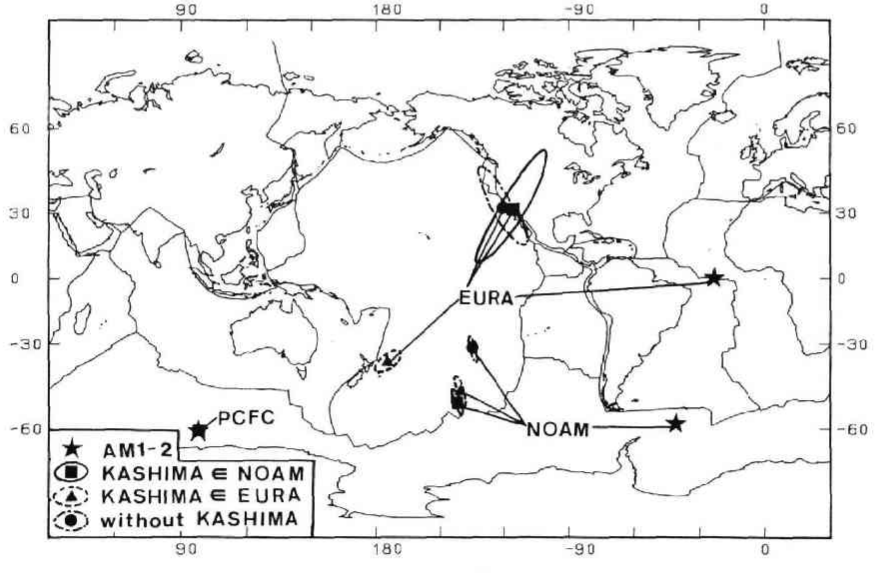

Fig. 5 Pole positions of PCFC, NOAM and EURA obtained by the inversions of the changing rates of the VLBI baseline lengths. Approximate 1-sigma error ellipses of each pole position are also drawn. The pole positions of these plates in the AM1-2 model (Minster and Jordan, 1978) are also depicted for comparison. The pole position of PCFC is fixed to that of the AM1-2model.

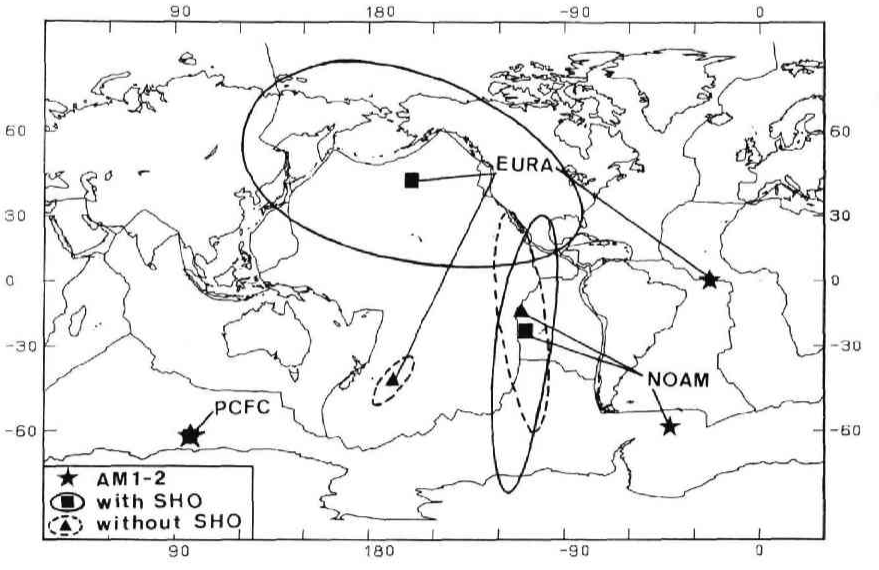

Fig. 6 The same as Fig. 5, but obtained by the inversions of the changing rates of the SLR baseline lengths.

plate motion parameters deduced here from the VLBI and SLR data sets are considered to be appropriate for recent years. On the other hand, those of the AM1-2 model are averaged over a geological time scale, that is, a few million years. Therefore, this inconsistency of the parameters suggests that the plate motions in recent years are different from those averaged over a geological time span.

Next, looking in detail, we are also aware that the estimated parameters of EURA seem to change from case to case much more than those of NOAM in both of the inversions of the VLBI and SLR data sets.

For example, in the inversions of the VLBI data sets, the parameters of EURA change significantly, depending on if the KASHIMA station belongs to NOAM (data set ; VLBI-56) or EURA (data set ; VLBI-59). However, those of NOAM do not change so much. This may be principally due to that the KASHIMA station is located in a plate margin in any case where it belongs to NOAM or EURA. The differences in the parameters of EURA from case to case are much larger than their 1-sigma formal errors so that we may regard these differences are meaningful. Moreover, the parameters estimated from VLBI-51 (without the KASHIMA station) are also slightly different from those estimated in these two cases. It may be roughly said that the parameters of NOAM estimated from VLBI-51 are closer to those estimated from VLBI-59. On the other hand, the parameters of EURA estimated from VLBI-51 are closer to those estimated from VLBI-56. The set of parameters derived from VLBI-51 may be preferred, provided that the KASHIMA station is indeed much affected by intraplate deformation. It is, however, impossible at present to judge exactly which set of parameters reflects the real plate motions. Consequently, we cannot say on which plate the

KASHIMA station exists.

As to the results obtained from the SLR data sets, two parameters change drastically, depending on if the data set includes (data set ; SLR-54) or excludes (data set ; SLR-47) the SHO (7838) station. These parameters are the latitude of the rotation pole and the rotation rate of EURA. It is again hard to decide which set of parameters is close to the reality. However, if it is true that the SHO (7838) station is much affected by intraplate deformation, we may prefer the set of parameters obtained from SLR-47.

6. Discussion and Conclusions

The changing rates of VLBI and SLR baseline lengths have been inverted by a conventional least squares method to estimate the plate motion parameters of NOAM and EURA.

We used the changing rates data of about 60 VLBI baselines out of more than 190 baselines given in Ma *et al.* (1989). We chose these baselines according to the following criteria : (1) The baselines should be interplate, and (2) for each baseline there should be at least five observations spanning at least two years after 1983. We also rejected the baselines including the HARTRAO station which is the only one on the African plate.

Almost all changing rates of thus selected baseline lengths were clearly found to be smaller than the rates expected from the AM1-2 model. This is the most striking feature of the changing rates of baseline lengths observed by VLBI. On the other hand, about two-thirds of the changing rates of baseline lengths observed by SLR, which were taken from Murata (1988), were larger than the rates expected from the same model. This contradiction in the changing rates data obtained from VLBI and SLR observations must be significantly reflected to the inverted results. From the results tabulated in Table 4, it is found that this contradicition seems to be reflected much more to the pole position of each plate than to the rotation rate. The sets of baselines in the VLBI and SLR data sets are not exactly same. Furthermore, even for the baselines included in both of the VLBI and SLR data sets, the ratios of the changing rates of corresponding baselines obtained with VLBI and SLR are not constant. Therefore, the contradiction in the changing rates data of VLBI and SLR does not simply affect only the rotation rate of each plate, but affects both of the pole position and rotation rate. Anyway, the reason of this contradiction should be investigated intensively in the future ; this is beyond the target of the present study.

Moreover, the discrepancy between the changing rates of baseline lengths observed by VLBI or SLR and those expected from the current plate motion model, the AM1-2 model, is very important to be interpreted geophysically. This discrepancy, of course, implies the inconsistency of recent plate motions with those averaged over a geological time scale.

We assumed that the changes of the baseline lengths are entirely caused by horizontal motions of rigid plates on the earth's surface. However, there must be vertical components in the displacement of observational stations which may affect more or less the estimated parameters. Furthermore, a possibility of uniform contraction of the

earth at a rate of 1.6×10^{-9}/yr (common downward movements of stations at a rate of 1.0 cm/yr) is recently suggested by Heki (1989). Such unmodeled effects in the present study should be also taken into account in the future. The effect of intraplate deformation upon the changing rates of the baseline lengths should be also considered. In particular, it should be taken into consideration if the baseline includes a station located in tectonically active regions such as the Japanese islands and the western part of the North American continent.

The numbers and distributions of observational stations of VLBI and SLR are not presently sufficient to estimate the parameters of all plates appearing in the AM1-2 model. Hence we could obtain the parameters of only two plates, namely, NOAM and EURA relative to PCFC. In the furure, it is expected that observational stations be distributed so that there are at least two stations on any known plate in order to construct a global plate motion model such as the AM1-2 model.

The results of simulations suggest that the standard deviation of observational errors in the changing rates data should be as small as 0.1 cm/yr to estimate the rotation pole and rotation rate of each plate with errors less than a few degrees and a few percent, respectively. In spite of much effort, such precision of observation is not yet achieved even by VLBI and SLR. However, one may expect that this high precision will be attained in the near future when the error sources affecting the VLBI and SLR measurements are taken away one by one (Carter and Robertson, 1989). In particular, correction to the so-called 'excess path delay' effect in the troposphere of the earth must be made to an enough extent.

Another problem lies in that something like a periodic variation with a period less than one year has been found in some baseline length changes (*e.g.*, Carter and Robertson, 1989). Its cause must be also clarified in order to make much precise estimation of the plate motion parameters.

The plate motion parameters estimated in the present study from the changing rates data of VLBI and SLR baseline lengths are considered to be affected by the factors mentioned above. Nevertheless, there are a few noteworthy points which should be emphasized.

(1) Some difference exists between the parameters of each plate estimated independently from the VLBI and SLR data sets.

(2) The estimated parameters of EURA seem to change much more than those of NOAM, depending on which plate includes the KASHIMA station, EURA or NOAM. It is, however, difficult to judge which set of parameters is close to the reality. Thus we cannot say at present to which plate the KASHIMA station, located in the northeastern part of the Japanese islands, belongs.

(3) Neither the parameters obtained from the VLBI data nor those obtained from the SLR data agree with the parameters of the AM1-2 model. This discrepancy between the parameters obtained in the present study and those of the AM1-2 model suggests that the plate motions in recent years are somewhat different from the ones averaged over a geological time scale. Therefore, it is geophysically important to

observe continuously the plate motions with VLBI and SLR in order to monitor them in a real-time sense.

Acknowledgments : The author would like to thank Drs. K. Yokoyama, K. Tanikawa and S. Manabe of the National Astronomical Observatory for valuable discussions and advice as well as for improvement of the manuscript. Thanks are also due to the referee for valuable comments.

References

Carter, W.E. and D.S. Robertson, 1989 : Definition of a terrestrial reference frame using IRIS VLBI observations : approaching millimeter accuracy, *Proc. 2nd Int. Assoc. Geod.*, Edinburgh, in press.

Chapman, M.E. and S.C. Solomon, 1976 : North American-Eurasian plate boundary in northeast Asia, *J. Geophys. Res.*, **81**, 921-930.

Chase, C.G., 1972 : The *N* plate problem of plate tectonics, *Geophys. J. R. astr. Soc.* **29**, 117-122.

Christodoulidis, D.C., D.E. Smith, R. Kolenkiewicz, S.M. Klosko, M.H. Torrence and P.J. Dunn, 1985 : Observing tectonic plate motions and deformations from satellite laser ranging, *J. Geophys. Res.*, **90**, 9249-9263.

Forsyth, D. and S. Uyeda, 1975 : On the relative importance of the driving forces of plate motion, *Geophys. J. R. astr. Soc.*, **43**, 163-200.

Goldstein, H., 1980 : *Classical Mechanics*, 2nd edition, Addison-Wesley, 606-610.

Heki, K., Y. Takahashi, T. Kondo, N. Kawaguchi, F. Takahashi and N. Kawano, 1987 : The relative movement of the North American and Pacific plates in 1984-1985, detected by the Pacific VLBI network, *Tectonophysics*, **144**, 151-158.

Heki, K., 1989 : Displacement of Kashima very long baseline interferometry station with respect to the North American plate, *J. Geod. Soc. Japan*, **35**, 97-104.

Heki, K., Y. Takahashi and T. Kondo, 1989 : The baseline length changes of circumpacific VLBI networks and their bearing on global tectonics, *IEEE Trans. Instrum. Meas.*, **38**, 680-683.

Kobayashi, Y., 1983 : On the initiation of subduction of plates, *Chikyu* (*The Earth Monthly*), **5**, 510-514 (in Japanese).

Kondo, T., K. Heki and Y. Takahashi, 1986 : Pacific plate motion detected by the VLBI experiments conducted in 1984-1985, *Proc. Symp. Appl. Space Tech. Astr. Geophys.*, Tokyo, 98-107.

Ma, C., J.W. Ryan and D. Caprette, 1989 : Crustal Dynamics Project data analysis-1988 ; VLBI geodetic results 1979-87, *NASA Tech. Memo., 100723*, Goddard Space Flight Center, Maryland.

Minster, J.B., T.H. Jordan, P. Molnar and E. Haines, 1974 : Numerical modelling of instantaneous plate tectonics, *Geophys. J.R. astr. Soc.*, **36**, 541-576.

Minster, J.B. and T.H. Jordan, 1978 : Present-day plate motions, *J. Geophys. Res.*, **83**, 5331-5354.

Murata, M., 1988 : Station coordinates, earth rotation and plate motions from LAGEOS laser ranging : 1983-1986, *J. Geod. Soc. Japan*, **34**, 33-57.

Nakagawa, T. and Y. Oyanagi, 1982 : *Analyses of experimental data by the least squares method-Program SALS*, Press Univ. Tokyo, Tokyo, pp. 206 (in Japanese).

Nakamura, K., 1983 : Possible nascent trench along the eastern Japan Sea as the convergent boundary between Eurasian and North American plates, *Bull. Earthq. Res. Inst. Univ. Tokyo*, **58**, 711-722 (in Japanese with English abstract).

Sasaki, M., 1989 : Station positions and plate motions derived by the SLR observations, *Abstr. 71st Meet. Geod. Soc. Japan*, No. 29 (in Japanese).

Wilkinson J.H. and C. Reinsch, 1971 : *Linear Algebra*, Springer-Verlag, 111-118.

Appendix. Calculation of the Jacobian Matrix A

Let the i-th baseline connect the station-a on plate-k and station-b on plate-l. Then the theoretical changing rate of this baseline length Π_i is given by the right-hand-side of (5) in section 2.1:

$$\Pi_i = | \boldsymbol{F}_k \boldsymbol{x}_a - \boldsymbol{F}_l \boldsymbol{x}_b | - | \boldsymbol{x}_a - \boldsymbol{x}_b |, \tag{A-1}$$

where $\boldsymbol{x}_c = (x_c, y_c, z_c)^t$ $(c = a, b)$ is given by (1) and $\boldsymbol{F}_q$ $(q = k, l)$ by (3) together with (4). Here t means transposition. The elements of the Jacobian matrix $\boldsymbol{A}$ are given by $A_{ij} = \partial \Pi_i / \partial m_j (i = 1 \sim N_o,\ j = 1 \sim 3(N_p - 1))$, where m_j means the j-th component of the model vector $\boldsymbol{m}$ and N_o is the number of baselines.

Thus we can calculate the elements of $\boldsymbol{A}$ as follows:

$$\left.\begin{array}{ll} A_{ij} = | \boldsymbol{x}'_{ab} |^{-1} \boldsymbol{x}'_{ab} \partial \boldsymbol{x}'_a / \partial m_j, & \text{if } 3k-2 \le j \le 3k, \\ A_{ij} = - | \boldsymbol{x}'_{ab} |^{-1} \boldsymbol{x}'_{ab} \partial \boldsymbol{x}'_b / \partial m_j, & \text{if } 3l-2 \le j \le 3l, \\ A_{ij} = 0, & \text{otherwise}, \end{array}\right\};\ i = 1 \sim N_o,\ j = 1 \sim 3(N_p - 1), \tag{A-2}$$

where

$$\boldsymbol{x}'_{ab} = (x'_a - x'_b,\ y'_a - y'_b,\ z'_a - z'_b), \tag{A-3}$$

and $| \boldsymbol{x}'_{ab} |$ must not be zero. Here $\boldsymbol{x}'_c = (x'_c, y'_c, z'_c)^t$ $(c = a, b)$ is given by (2).

From (2),

$$\frac{\partial \boldsymbol{x}'_c}{\partial m_j} = \frac{\partial \boldsymbol{F}_q}{\partial m_j} \boldsymbol{x}_c, \tag{A-4}$$

where c is either a or b, and $q = k$ when $c = a$ whereas $q = l$ when $c = b$.

From (3), we obtain

$$\frac{\partial \boldsymbol{F}_q}{\partial m_j} = \begin{pmatrix} \partial f_{11}(\Phi_q, \Lambda_q, \Omega_q)/\partial m_j & \partial f_{12}(\Phi_q, \Lambda_q, \Omega_q)/\partial m_j & \partial f_{13}(\Phi_q, \Lambda_q, \Omega_q)/\partial m_j \\ \partial f_{21}(\Phi_q, \Lambda_q, \Omega_q)/\partial m_j & \partial f_{22}(\Phi_q, \Lambda_q, \Omega_q)/\partial m_j & \partial f_{23}(\Phi_q, \Lambda_q, \Omega_q)/\partial m_j \\ \partial f_{31}(\Phi_q, \Lambda_q, \Omega_q)/\partial m_j & \partial f_{32}(\Phi_q, \Lambda_q, \Omega_q)/\partial m_j & \partial f_{33}(\Phi_q, \Lambda_q, \Omega_q)/\partial m_j \end{pmatrix}, \tag{A-5}$$

where, from (4),

$$\left.\begin{array}{l} \partial f_{11}/\partial \Phi = 2 \cos \Phi \sin \Phi \cos^2 \Lambda (\cos \Omega - 1), \\ \partial f_{12}/\partial \Phi = 2 \cos \Phi \sin \Phi \cos \Lambda \sin \Lambda (\cos \Omega - 1) - \cos \Phi \sin \Omega, \\ \partial f_{13}/\partial \Phi = \cos \Lambda (\sin^2 \Phi - \cos^2 \Phi)(\cos \Omega - 1) - \sin \Phi \sin \Lambda \sin \Omega, \\ \partial f_{21}/\partial \Phi = 2 \cos \Phi \sin \Phi \cos \Lambda \sin \Lambda (\cos \Omega - 1) + \cos \Phi \sin \Omega, \\ \partial f_{22}/\partial \Phi = 2 \cos \Phi \sin \Phi \sin^2 \Lambda (\cos \Omega - 1), \\ \partial f_{23}/\partial \Phi = \sin \Lambda (\sin^2 \Phi - \cos^2 \Phi)(\cos \Omega - 1) + \sin \Phi \cos \Lambda \sin \Omega, \\ \partial f_{31}/\partial \Phi = \cos \Lambda (\sin^2 \Phi - \cos^2 \Phi)(\cos \Omega - 1) + \sin \Phi \sin \Lambda \sin \Omega, \\ \partial f_{32}/\partial \Phi = \sin \Lambda (\sin^2 \Phi - \cos^2 \Phi)(\cos \Omega - 1) - \sin \Phi \cos \Lambda \sin \Omega, \\ \partial f_{33}/\partial \Phi = -2 \sin \Phi \cos \Phi (\cos \Omega - 1), \end{array}\right\} \tag{A-6}$$

$$
\left.\begin{aligned}
&\partial f_{11}/\partial \Lambda = 2\cos^2 \Phi \cos \Lambda \sin \Lambda(\cos \Omega - 1),\\
&\partial f_{12}/\partial \Lambda = \cos^2 \Phi(\sin^2 \Lambda - \cos^2 \Lambda)(\cos \Omega - 1),\\
&\partial f_{13}/\partial \Lambda = \cos \Phi \sin \Phi \sin \Lambda(\cos \Omega - 1) + \cos \Phi \cos \Lambda \sin \Omega,\\
&\partial f_{21}/\partial \Lambda = \cos^2 \Phi(\sin^2 \Lambda - \cos^2 \Lambda)(\cos \Omega - 1),\\
&\partial f_{22}/\partial \Lambda = -2\cos^2 \Phi \cos \Lambda \sin \Lambda(\cos \Omega - 1),\\
&\partial f_{23}/\partial \Lambda = -\cos \Phi \sin \Phi \cos \Lambda(\cos \Omega - 1) + \cos \Phi \sin \Lambda \sin \Omega,\\
&\partial f_{31}/\partial \Lambda = \cos \Phi \sin \Phi \sin \Lambda(\cos \Omega - 1) - \cos \Phi \cos \Lambda \sin \Omega,\\
&\partial f_{32}/\partial \Lambda = -\cos \Phi \sin \Phi \cos \Lambda(\cos \Omega - 1) - \cos \Phi \sin \Lambda \sin \Omega,\\
&\partial f_{33}/\partial \Lambda = 0,
\end{aligned}\right\} \qquad \text{(A-7)}
$$

and

$$
\left.\begin{aligned}
&\partial f_{11}/\partial \Omega = -\sin^2 \Phi \cos^2 \Lambda \sin \Omega - \sin^2 \Lambda \sin \Omega,\\
&\partial f_{12}/\partial \Omega = \cos^2 \Phi \cos \Lambda \sin \Lambda \sin \Omega - \sin \Phi \cos \Omega,\\
&\partial f_{13}/\partial \Omega = \cos \Phi \sin \Phi \cos \Lambda \sin \Omega + \cos \Phi \sin \Lambda \cos \Omega,\\
&\partial f_{21}/\partial \Omega = \cos^2 \Phi \cos \Lambda \sin \Lambda \sin \Omega + \sin \Phi \cos \Omega,\\
&\partial f_{22}/\partial \Omega = -\sin^2 \Phi \sin^2 \Lambda \sin \Omega - \cos^2 \Lambda \sin \Omega,\\
&\partial f_{23}/\partial \Omega = \cos \Phi \sin \Phi \sin \Lambda \sin \Omega - \cos \Phi \cos \Lambda \cos \Omega,\\
&\partial f_{31}/\partial \Omega = \cos \Phi \sin \Phi \cos \Lambda \sin \Omega - \cos \Phi \sin \Lambda \cos \Omega,\\
&\partial f_{32}/\partial \Omega = \cos \Phi \sin \Phi \sin \Lambda \sin \Omega + \cos \Phi \cos \Lambda \cos \Omega,\\
&\partial f_{33}/\partial \Omega = -\cos^2 \Phi \sin \Omega.
\end{aligned}\right\} \qquad \text{(A-8)}
$$